Formation of a two-dimensional oxide via oxidation of a layered material

Luca Camilli,[a] Daniele Capista,[b] Massimo Tomellini,[c] Jianbo Sun,[d,e] Patrick Zeller,†[f] Matteo Amati[f], Luca Gregoratti,[f] Luca Lozzi[b] and Maurizio Passacantando[b]*

ABSTRACT. We investigate the oxidation mechanism of the layered model system GeAs. In situ X-ray photoelectron spectroscopy experiments performed by irradiating an individual flake with synchrotron radiation in presence of oxygen show that while As leaves the GeAs surface upon oxidation, a Ge-rich ultrathin oxide film is being formed in the topmost layer of the flake. We develop a theoretical model that supports the layer-by-layer oxidation of GeAs, with a logarithmic kinetics. Finally, assuming that the activation energy for the oxidation process changes linearly with coverage, we estimate that the activation energy for As oxidation is almost twice that for Ge at room temperature.

A Introduction

Lately, ultrathin oxide films have been emerging as a promising new class of two dimensional (2D) materials. Among them, silica or germania single- and bi-layer have attracted much attention as they show tuneable crystallinity, ranging from a highly ordered crystal state to a complete amorphous one, depending on the growth characteristics[1]. In particular, the structure of the amorphous state has been widely investigated at the atomic level revealing interesting information on the structure and the dynamics of glassy and disordered materials at low dimensions[2,3]. The preparation of these films is rather challenging and still not scalable, and although there is a report where 2D silica has been obtained on graphene, in the other cases the ultra-thin oxide films have been grown on metallic surfaces (like Ru(0001) or Mo(112))[4–6]. Furthermore, it is still unclear whether this method could be used to form 2D oxides of, for example, transition metals, for the synthesis of which other processes can be used[7,8]. In this work, we explore a possible alternative approach for the formation of an ultra-thin 2D oxide film, namely the oxidation of a parent layered material. Indeed, excluding graphene and hexagonal boron nitride, most layered materials are somewhat unstable at environmental conditions. Some, like black phosphorus for example, if left in air will quickly and severely degrade[9]; others, like GeAs and GeS_2, will form an ultra-thin oxide passivating layer on their surface that eventually prevents oxidation of the inner layers[10]. Even transition metal dichalcogenides, which have long been thought to be stable in air, will react with oxygen over time, starting at chalcogen vacancy sites[11,12]. Despite this, detailed information about the atomistic mechanism leading to two-dimensional oxidation of layered materials is still lacking.

In this study, we try to fill this knowledge gap by taking GeAs as layered model system. Notably, we focus on the first stages of the oxidation process that leads to the formation of a 2D oxide layer, and provide novel and detailed insights into its mechanism and kinetics. The oxidation experiment has been performed at in situ conditions on a single GeAs flake using synchrotron radiation, which allowed us to gain accurate chemical information about the sample surface at the single flake level via X-ray photoelectron spectromicroscopy (that is, spatially resolved X-ray photoelectron spectroscopy, XPS). The data show that the oxidation process is rather slow and confined to the topmost GeAs layer. Notably, As in this layer abandons the surface as gas upon reacting with oxygen, whereas a solid Ge-rich 2D film is being formed. Furthermore, we have developed a theoretical model that explains well the time dependence of Ge and As XPS intensity signals, hence providing useful insights into the kinetics of the oxidation reaction.

B Experimental

GeAs flakes were deposited from a single crystal (2D Semiconductors) using scotch tape method on a 2-nm-Au-coated Si/SiO_2 substrate with index marks. The XPS experiments were carried out at the ESCA Microscopy beamline at Elettra[13] (Trieste, Italy) with photon energy of 647.95 eV, pass energy of 20 eV, detection angle of 30° with respect to the sample surface and an X-ray beam of 130 nm diameter. To avoid any contamination of the sample, the exfoliation was carried out in the UHV chamber ($p < 7\times10^{-10}$ mbar). Photoelectron maps of Ge 3d were acquired to localize suitable, isolated flakes (Figure 1). Prior to starting the oxidation experiment, a survey spectrum was acquired to confirm the absence of oxygen and other contaminants on the flake's surface. Next, a small amount of oxygen was let into the chamber via a leak valve (oxygen partial pressure being 1.75×10^{-6} mbar), while Ge 3d and As 3d core levels were collected continuously to follow the formation of the ultrathin oxide layer at in situ conditions. Being relatively close in binding energy, Ge 3d and As 3d were both collected within a single spectrum-sweep. This simple choice guarantees that the two spectra are always normalized to each other. All spectra shown here are energy calibrated with respect to the position of Au $4f_{7/2}$ photoelectrons (binding energy, BE = 84.0 eV) of an Au reference sample. After the experiments at Elettra, the same flakes were characterized ex situ by optical microscopy and atomic force microscopy (AFM) (Figure 1).

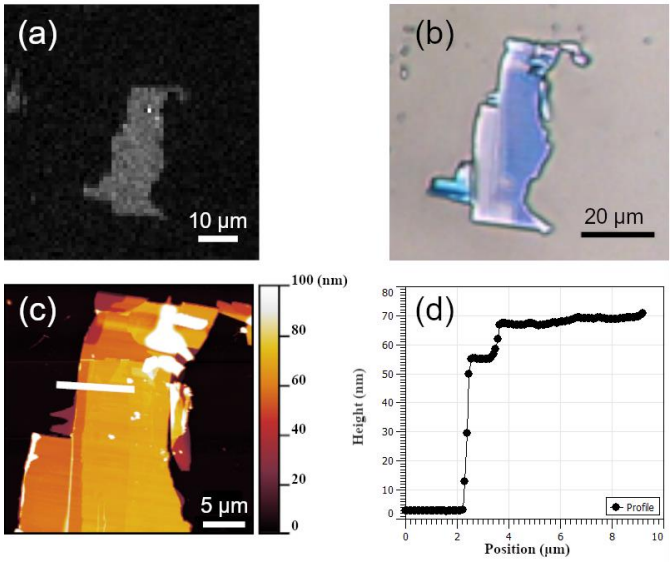

Figure 1. (a) Ge 3d map of a flake selected for the *in situ* oxidation experiment. (b) Optical image and (c) AFM image of the same GeAs flake. (d) Thickness profile along the white line in the AFM image in (c).

C Results and discussion

Figure 2a shows the different behaviour of Ge and As in GeAs upon exposure to oxygen. The intensity of As 3d peak displays only a continuous intensity reduction, without any apparent change of the line shape, while the Ge 3d peak shows also a broadening due to the formation of a shoulder at higher binding energy. The spectra have been fitted using two components for As 3d and five components for Ge 3d[14,15] as reported in Figure 2b.

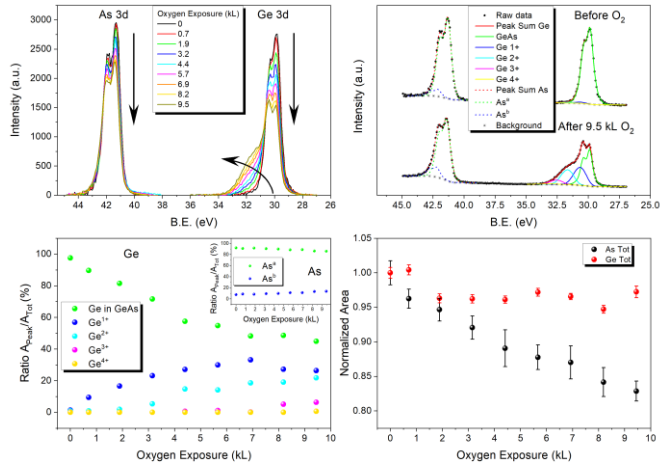

Figure 2. (a) Ge 3d and As 3d spectra of GeAs flake during an oxidation experiment. (b) Fitted spectra of Ge 3d and As 3d at the beginning and at the end of the oxidation. (c) Evolution of the ratio of the area of individual components in Ge 3d and As 3d (insert) to the total area of the peak during the oxidation. (d) Evolution of the total area of the Ge 3d and As 3d peaks normalized to the peak area before the oxidation. The error bars represent the uncertainty in the fit.

The five components of germanium are the characteristic doublet of GeAs (BE = 29.9 eV), followed by the different oxidation states of Ge, that is Ge^{1+} (BE = 30.5 eV), Ge^{2+} (BE = 31.5 eV), Ge^{3+} (BE = 32.4 eV), Ge^{4+} (BE = 33 eV)[14]; the two components of As are instead the one from As-Ge bond (As^a, BE = 41.3 eV) and the one from As-As (As^b, at BE = 42.1 eV)[15,16]. The evolution of the individual components in Ge 3d and As 3d core levels are reported in
Figure 2c. Prior to introducing oxygen in the chamber, germanium shows only the components characteristic of GeAs (notice the sharp peak in the upper spectrum of Figure 2b), whereas, upon oxidation, new components appear at higher binding energy, as a result of bonds with oxygen. It is worth noting that in our experiments germanium never reaches the oxidation state of Ge^{4+} characteristic of bulk GeO_2 (note the intensity of the yellow, solid line in Figure 2b). Also, after about 7000 Langmuir (L) of oxygen a plateau is reached, and the area of the unoxidized Ge component has decreased to 45% of its initial value. On the other hand, the two As components – that is, As^a and As^b – show only a minor change over time, with As^a intensity slowly decreasing and As^b slowly increasing (note the Inset in Figure 2c), possibly indicative of As dimerization[17]. Lastly, Figure 2d reports the evolution of the total area of Ge 3d and As 3d core levels throughout the experiment (after normalization with the peak area before oxidation). By looking at this graph it is possible to have a better understanding of what is happening in the sample. The total Ge area, apart from small fluctuations, remains constant during the experiment, indicating that the total amount of germanium inside the sample is not changing over time. Simply, some of the Ge in GeAs is now forming new bonds with oxygen. The As area is instead clearly decreasing (as it was already visible in Figure 2a), revealing that arsenic is being lost during the oxidation of GeAs. A similar behaviour was also observed during oxidation of As-terminated silicon[17]. Notably, at the end of the experiment, approximately 17% of As in the sampled volume has been lost. Considering the kinetic energy of the Ge 3d and As 3d photoelectrons and the detection angle in our experimental setup, we can estimate the escape depth in our experiments as to 2.22 nm (the escape depth if defined as 3 times the effective IMFP, see Supplementary Information), which provides a sampling thickness of a bit more than 3 GeAs layers (the interlayer distance in GeAs being 0.66 nm). By taking into account the exponential attenuation of the XPS intensity with respect to the distance from the surface, from our data we can infer that almost all of the Ge atoms in the

first GeAs monolayer have reacted with oxygen (see Supplementary Information).

The experimental data presented in Fig. 2 give us the possibility to propose a model for both oxidation kinetics and attenuation of the photoelectron intensity in the sample. In particular, the photoelectron intensity from oxidized (unoxidized) components are estimated by summing up the contributions arising by each layer and considering an attenuation factor depending on the electron mean free path, which has been taken as a constant over the whole oxidation reaction. Following the experimental data, we assume that the total number of Ge atoms in the sample is conserved during oxidation (see Fig. 2d), whereas As leaves the sample at a rate that is equal to its oxidation rate, namely *r*, with *r* being the rate of the reaction $\mathrm{As} + (x/2)\ \mathrm{O}_2 \rightarrow \mathrm{AsO}_x$. Within the framework of this model, we simplify the arrangement of Ge and As atoms in each GeAs monolayer (ML) as displayed in Figure 3. Namely, we consider each GeAs ML to be made up of five layers, two of As, the topmost and bottommost, and three of Ge, in the middle. Thus, we introduce two characteristic distances, *d* and *δ*, with *a* = *d*+*δ* being the distance between two consecutive GeAs MLs. To simplify the mathematical computation, in the following treatment the distance between two successive layers within the GeAs ML is taken equal to $d_1 = d/4$. The distance of each layer from the top layer, is then given by:

$$\mathrm{Ge-layers:}\quad d_{l,m} = (m-1)a + l d_1\ ;\ l = 1,2,3 \quad (1)$$

$$\mathrm{As-layers:}\ d_{l,m} = (m-1)a + (l-1)d\ ;\ \ l = 1,2 \quad (2)$$

In these equations *m* = 1,2,3... is the ML index, while *l* enumerates the Ge and As layers within the *m*-th GeAs ML. In what follows, the density of Ge (As) atoms in each layer of Ge (As) is assumed to be the same.

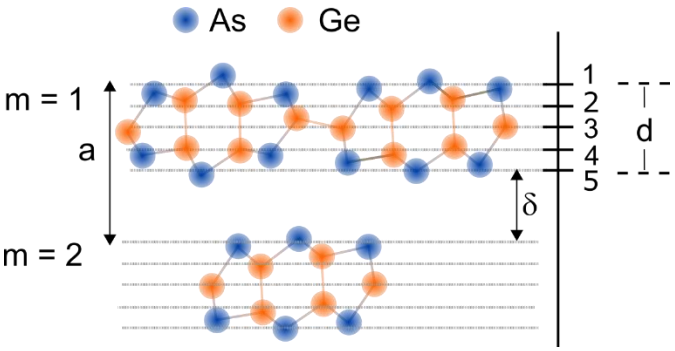

Figure 3. Sketch highlighting the geometrical parameters used for developing the kinetic model; *m* stems for the GeAs ML index, *δ* is the space between two consecutive MLs, *d* the ML thickness and *a* the distance between two consecutive GeAs ML. We approximate each GeAs ML with 5 layers (1 to 5); the topmost and bottommost layers are made of As (blue dots), the three middle ones by Ge (orange dots). More details can be found in the main text. a = 0.66 nm; d = 0.48 nm; δ = 0.18 nm.

The photoelectron intensity from an oxidized Ge layer at $d_{l,m}$ is attenuated by a factor of $e^{-d_{l,m}/\lambda}$. Therefore, the whole photoelectron intensity, due to *n* oxidized MLs plus *j* Ge layers underneath (*j* ≤ 3), reads:

$$I_{\mathrm{Ge},ox} = I_0\left[\left(\sum_{k=0}^{n-1} e^{-ka/\lambda}\right)\left(\sum_{l=1}^{3} e^{-ld_1/\lambda}\right) + e^{-na/\lambda}\sum_{l=1}^{j} e^{-ld_1/\lambda}\right] \quad (3)$$

with I_0 the intensity from a single layer of Ge in the oxide placed at *d* = 0. The first term of the square bracket accounts for the three Ge layers (thus, the sum over *l*) of the fully oxidized *n* GeAs MLs. In the first round-bracket, each term in the sum over *k* refers to the distance (including *δ*) of the (*k*+1)st fully-oxidized ML from the flake surface (that is, the distance *ka*). The second term of the equation considers, instead, the partially oxidized GeAs ML within the (*n*+1)st ML. Obviously, when none of the GeAs MLs is fully oxidized, then *n* = 0 and the first contribution in the square bracket vanishes. From eqn. 3, it stems that the photoelectron intensity is a function of *n* and *j*: $I_{\mathrm{Ge},ox} \equiv I(n,j)$, where $I(n,3) = I(n+1,0)$.

Eqn. 3 can be rewritten as

$$I_{\mathrm{Ge},ox} = I_0\left[\left(\frac{1-X^n}{1-X}\right)A + X^n F(j)\right] \quad (4)$$

with $X = e^{-a/\lambda}$, $F(j) = \sum_{l=1}^{j} e^{-ld_1/\lambda}$ and $A = F(3) = \sum_{l=1}^{3} e^{-ld_1/\lambda}$. The thickness of the oxide, expressed in number of Ge-layers, is equal to *J* = 3*n* + j, where *J* is to be considered time dependent (see eqn. 8 below).

Considering the same cross-sections for the oxidized and unoxidized components, the intensity from the unoxidized Ge ($\mathrm{Ge}^{(0)}$) is

$$I_{\mathrm{Ge}^{(0)}} = I_0 \left[e^{-na/\lambda} \sum_{l=j+1}^{3} e^{-ld_1/\lambda} + \sum_{l=1}^{3} e^{-ld_1/\lambda} \sum_{k=n+1}^{\infty} e^{-ka/\lambda} \right] \quad (5)$$

where the first term of the squared bracket accounts for the yet unoxidized Ge (thus the sum over *l*+1) in the last oxidized GeAs ML (that is, the *n*+1 layer), whereas the second term accounts for the signal from the unoxidized GeAs MLs.

Eqn. 5 can be rewritten as

$$I_{\mathrm{Ge}^{(0)}} = I_0 \left[X^n \big(A - F(j)\big) + A \frac{X^{n+1}}{1-X} \right] \quad (6)$$

To interpret the experimental data, we normalize the intensities according to $I'_{\mathrm{Ge}^{(0)}} + I'_{\mathrm{Ge},ox} = 1$. From eqns. 4 and 6 it follows that $I_{\mathrm{Ge}^{(0)}} + I_{\mathrm{Ge},ox} = \frac{I_0 A}{1-X}$. Accordingly, the intensities are divided by the factor $\frac{I_0 A}{1-X}$. For the $\mathrm{Ge}^{(0)}$ component the normalized intensity is

$$I'_{\mathrm{Ge}^{(0)}} = X^n - X^n(1-X)\frac{y - y^{j+1}}{y - y^4} = X^n - X^n(1-X)\frac{1-y^j}{1-y^3} \quad (7)$$

where $\boldsymbol{y = e^{-d_1/\lambda}}$. Eqn. 7 gives the number of oxidized layers within the (*n*+1)-th ML:

$$j = -\frac{\lambda}{d_1} \ln \left[\frac{I'_{\mathrm{Ge}^{(0)}} - X^n}{X^n(1-X)} (1 - y^3) + 1 \right]. \quad (8)$$

Eqn. 8 can be used for determining the time dependence of the number of oxidized layers from the experimental XPS intensities, with the parameter values being $\lambda = 0.75$ nm, d_1 = 0.12 nm and a = 0.66 nm. The "kinetics" has been computed by assuming n = 0,1,... full oxidized MLs.‡

The outcome of the computation shows that *n* is equal to zero in the considered time interval (0 – 120 min). The whole number of layers, *J*, increases up to a maximum of 2.8 (Figure 4). Therefore, the present analysis is confirming that the whole oxidation process involves just one GeAs ML, approximatively. It is worth to point out that also in a previous study of ours, in which we exploited the spontaneous oxidation of GeAs (as well as of GeS_2) in environmental conditions to develop a layer-by-layer thinning technique[10], only the top GeAs monolayer was involved in the oxidation reaction.

A similar approach is also applied to As. In this case, As photoelectron intensity from the sample decreases over time, as explained above. The normalized photoelectron intensity can be written with an equation similar to eqn. 7 above (see Supplementary Information for more details):

$$I'_{\mathrm{As}^{(0)}} = \left[\frac{1-X}{B} X^n \big(B - G(j)\big) + X^{n+1} \right], \quad (9)$$

where $B = 1 + z$, $z = e^{-d/\lambda}$ and $G(j) = \sum_{l=1}^{j} e^{-(l-1)d/\lambda} = \sum_{m=0}^{j-1} z^m$ with $j \leq 2$. By using the identity $\frac{G(j)}{B} = \frac{1-z^j}{1-z^2}$, the number of oxidized layers of As within the (*n*+1)-th ML (hence, removed from the surface) is given by

$$j = -\frac{\lambda}{d} \ln \left[\frac{I'_{\mathrm{As}^{(0)}} - X^n}{X^n(1-X)} (1 - z^2) + 1 \right]. \quad (10)$$

Using the experimental XPS intensity of As 3d core level, eqn. 10 can be employed to obtain the number of As layers removed from the GeAs flake. In this case we get a value of *J* that is lower than one (Figure 4). This outcome should be interpreted in the framework of a kinetic approach; specifically, the ratio between an increment of J and the elapsed time, $\Delta J/\Delta t$, gives the mean oxidation rate expressed in As-layer per unit time.

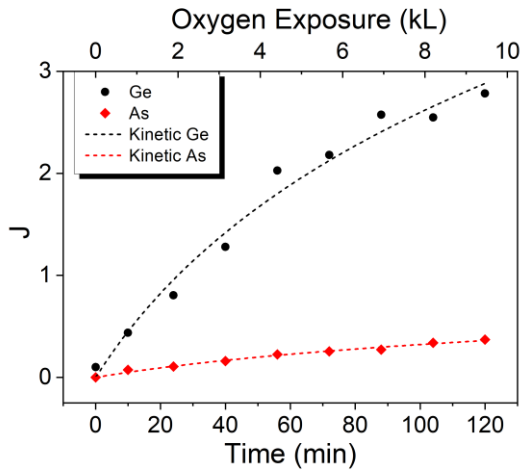

Figure 4. Time evolution of the number of Ge and As layers involved in the oxidation process. The points (dots for Ge and diamonds for As) in the graph are the experimental data of the non-oxidized Ge (already shown in Fig. 2c) and of the total As photoelectron intensity (already shown in Fig. 2d) properly modified. The dashed lines are the best fit obtained with a logarithmic kinetic law (see main text for more details). For Ge, $J = 3n + j$ with n being the number of GeAs MLs in which all Ge atoms have reacted with oxygen, and $j \leq 3$; for As, $J = 2n' + j$ with n' being the number of GeAs MLs in which all As atoms have reacted with oxygen, and $\boldsymbol{j \leq 2}$

Therefore, we next attempt to describe the oxidation kinetics. Kinetic data on the oxidation of GeAs are lacking in literature at odds with the oxidation of Germanium that has been investigated in a certain detail. In ref. 18, for example, the oxidation of Ge was studied in a wide interval of temperature and oxide thicknesses. It was demonstrated that in the early stage, the oxidation is in accord with the logarithmic law up to two monolayer thickness. At this point oxidation stops for an extended interval of time (which is temperature dependent). The logarithmic rate is derived by considering a process with activation energy that changes linearly with coverage. Integration of the rate equation provides the kinetics: $q(t) = \alpha \ln[1 + \beta t]$ where $q(t)$ is the number of oxidized atoms per unit surface with α and β depending on temperature[§]. The logarithmic kinetics is usually satisfied in the very early stage of metal-oxide formation at low and intermediate temperatures[19]. The best fit of the logarithmic kinetics to the data is shown in Figure 4 for Ge and As. The fitting parameters are $\alpha_{Ge} = 2.2$, $\alpha_{As} = 0.37$, $\beta_{Ge} = 0.023$ min^{-1} and $\beta_{As} = 0.014$ min^{-1}. From the logarithmic kinetics[§], we obtain $\frac{\gamma_{As}Q_{As}}{\gamma_{Ge}Q_{Ge}} = \frac{\beta_{As}}{\beta_{Ge}}$ and $\frac{\gamma_{As}}{\gamma_{Ge}} = \frac{\alpha_{Ge}}{\alpha_{As}}$, which allows one to estimate the difference between the activation energies for oxidation of Ge and As:

$$(E^*_{0,As} - E^*_{0,Ge}) = k_B T \ln\left(\frac{Q_{Ge}}{Q_{As}}\right) = k_B T \ln\left(\frac{\alpha_{Ge}\beta_{Ge}}{\alpha_{As}\beta_{As}}\right) = 2.28 k_B T.$$

If we assume an activation energy for Ge oxidation of 1580 cal/mol of O atom[18], the activation energy for As oxidation in our experimental conditions turns out to be approximately twice that for Ge at room temperature.

Conclusions

We have studied the oxidation of an individual GeAs flake of 66 nm thickness. The oxidation experiment has been carried out in situ at oxygen partial pressure of 1.75 x 10^{-6} mbar inside the ESCA microscopy beamline at ELETTRA (Trieste, Italy), while the spatially-resolved XPS signals of As 3d and Ge 3d were continuously collected. The data show that some of As leaves the GeAs as gas upon oxidation, while a Ge-rich oxide layer is being formed. We have constructed a model that replicates the evolution of the photoelectron intensities with time. By fitting experimental photoelectron intensities with the theoretical equations, we conclude that the oxidation involves only the very first GeAs ML (that is, the topmost one), where all the Ge atoms and much of the outmost As atoms have been reacting with oxygen. Although the model is very simple, and based on several approximations (for example, structural changes in GeAs due to oxidation are not taken into account and the mean free path is kept constant), the given interpretation – namely, formation of a ultrathin 2D oxide layer – finds support in light of previous studies performed in environmental conditions[10]. Moreover, by assuming that the activation energy for the oxidation process changes linearly with coverage, we estimate that the activation energy for As oxidation is almost twice that for Ge in our experimental conditions. 2D oxides have been recently emerging as new class of 2D materials with potential applications ranging from catalysis to energy generation, and the controlled oxidation of a layered material is potentially an alternative method for obtaining ultra-thin 2D oxide films. In this framework, the results reported here, providing novel insights into oxidation mechanism and kinetics of GeAs (and by extension, possibly of other layered materials too, such as GeS_2[10]) will be highly beneficial.

Author Contributions

The manuscript was written through contributions of all authors. All authors have given approval to the final version of the manuscript.

Conflicts of interest

There are no conflicts to declare.

Acknowledgements

This research is supported by the Villum Fonden through the Young Investigator Program (Project No. 19130). L.C. acknowledges support from the Italian Ministry of Education, University and Research (MIUR) via "Programma per Giovani Ricercatori - Rita Levi Montalcini 2017". The authors are thankful to Prof. M. Palummo and Prof. G. Giorgi for the fruitful discussions.

Notes and references

‡ In eqn. 8, because of the time dependence of $I'(t)$, $j \equiv j(t,n)$. The total number of oxidized layers at time t is $J(t) = \sum_{n=0}^{\infty}[3n + j(t,n)]H\big(3 - j(t,n)\big)H\,(j(t,n))$, with $H(\cdot)$ being the Heaviside step function ($H = 0$ for $x < 0$, $H = 1/2$ for $x = 0$ and $H = 1$ for $x > 0$).

§ The rate is given by $dq/dt = K(T,q) = \nu_0 \exp(-E^*(q)/k_B T)$, where q is the number of oxidized atoms and $E^*(q)$ the activation energy. A linear dependence of E^* with q implies $dq/dt = \nu_0 \exp(-(E_0^*(q) + \gamma q)/k_B T)$, with solution $q(t) = (k_B T/\gamma)\ln(1 + (Q\gamma/kBT)t)$, where $Q = \nu_0 \exp(-E_0^*(q)/k_B T)$.

1 A. L. Lewandowski, P. Schlexer, S. Tosoni, L. Gura, P. Marschalik, C. Büchner, H. Burrall, K. M. Burson, W.-D. Schneider, G. Pacchioni and M. Heyde, *J. Phys. Chem. C*, 2019, **123**, 7889–7897.
2 L. Lichtenstein, C. Büchner, B. Yang, S. Shaikhutdinov, M. Heyde, M. Sierka, R. Włodarczyk, J. Sauer and H.-J. Freund, *Angew. Chemie Int. Ed.*, 2012, **51**, 404–407.
3 P. Y. Huang, S. Kurasch, J. S. Alden, A. Shekhawat, A. A. Alemi, P. L. McEuen, J. P. Sethna, U. Kaiser and D. A. Muller, *Science (80-.).*, 2013, **342**, 224–227.
4 L. Lichtenstein, M. Heyde and H.-J. Freund, *Phys. Rev. Lett.*, 2012, **109**, 106101.
5 J. Weissenrieder, S. Kaya, J.-L. Lu, H.-J. Gao, S. Shaikhutdinov, H.-J. Freund, M. Sierka, T. K. Todorova and J. Sauer, *Phys. Rev. Lett.*, 2005, **95**, 76103.
6 P. Y. Huang, S. Kurasch, A. Srivastava, V. Skakalova, J. Kotakoski, A. V Krasheninnikov, R. Hovden, Q. Mao, J. C. Meyer, J. Smet, D. A. Muller and U. Kaiser, *Nano Lett.*, 2012, **12**, 1081–1086.
7 T. Yang, T. T. Song, M. Callsen, J. Zhou, J. W. Chai, Y. P. Feng, S. J. Wang and M. Yang, *Adv. Mater. Interfaces*, 2019, 6, 1801160.
8 Z. Sun, T. Liao, Y. Dou, S. M. Hwang, M. S. Park, L. Jiang, J. H. Kim and S. X. Dou, *Nat. Commun.*, 2014, 5, 3813.
9 J. O. Island, G. A. Steele, H. S. J. Van Der Zant and A. Castellanos-Gomez, *2D Mater.*, 2015, 2, 011002.
10 J. Sun, G. Giorgi, M. Palummo, P. Sutter, M. Passacantando and L. Camilli, *ACS Nano*, 2020, **14**, 4861–4870.
11 S. Barja, S. Refaely-Abramson, B. Schuler, D. Y. Qiu, A. Pulkin, S. Wickenburg, H. Ryu, M. M. Ugeda, C. Kastl, C. Chen, C. Hwang, A. Schwartzberg, S. Aloni, S. K. Mo, D. Frank Ogletree, M. F. Crommie, O. V. Yazyev, S. G. Louie, J. B. Neaton and A. Weber-Bargioni, *Nat. Commun.*, 2019, **10**, 1–8.
12 S. KC, R. C. Longo, R. M. Wallace and K. Cho, *J. Appl. Phys.*, 2015, **117**, 135301.
13 M. K. Abyaneh, L. Gregoratti, M. Amati, M. Dalmiglio and M. Kiskinova, *e-Journal Surf. Sci. Nanotechnol.*, 2011, **9**, 158–162.
14 A. Molle, M. N. K. Bhuiyan, G. Tallarida and M. Fanciulli, *Appl. Phys. Lett.*, 2006, **89**, 83504.
15 R. Suri, D. J. Lichtenwalner and V. Misra, *Appl. Phys. Lett.*, 2010, **96**, 112905.
16 S. Arabasz, E. Bergignat, G. Hollinger and J. Szuber, *Vacuum*, 2006, **80**, 888–893.
17 F. Rochet, C. Poncey, G. Dufour, H. Roulet, W. N. Rodrigues, M. Sauvage, J. C. Boulliard, F. Sirotti and G. Panaccione, *Surf. Sci.*, 1995, **326**, 229–242.
18 J. R. Ligenza, *J. Phys. Chem.*, 1960, **64**, 1017–1022.
19 K. R. Lawless, *Reports Prog. Phys.*, 1974, **37**, 231–316.